ELSEVIER

Clinical Neurophysiology 119 (2008) 1534–1545

www.elsevier.com/locate/clinph

Is it possible to automatically distinguish resting EEG data of normal elderly vs. mild cognitive impairment subjects with high degree of accuracy?

Paolo M. Rossini[a,b,c,*], Massimo Buscema[d], Massimiliano Capriotti[d], Enzo Grossi[e], Guido Rodriguez[f], Claudio Del Percio[g], Claudio Babiloni[a,b,h]

[a] *Associazione Fatebenefratelli per la ricerca (AFaR), S. Giovanni Calibita-Isola Tiberina, 00185 Rome, Italy*
[b] *Casa di Cura SAN RAFFAELE Cassino and IRCCS SAN RAFFAELE PISANA, Rome, Italy*
[c] *Neurology, Campus Biomedico University, Via Emilio Longoni, 83 – 00155 Rome, Italy*
[d] *Semeion Research Centre, Via Sersale, 117 – 00128, Rome, Italy*
[e] *Bracco SpA Medical Department, Via E. Folli, 50 – 20134, Milan, Italy*
[f] *Clinical Neurophysiology Service (DISEM), University of Genova, Italy*
[g] *Associazione Fatebenefratelli per la ricerca, Istituto di ricovero e cura a carattere scientifico S. Giovanni di Dio-Fatebenefratelli, 14 Via Piastroni, 4 – 2512 Brescia, Italy*
[h] *Dipartimento di Scienze Biomediche, Università di Foggia, Foggia, Italy*

Accepted 19 March 2008

Abstract

Objective: It has been shown that a new procedure (implicit function as squashing time, IFAST) based on artificial neural networks (ANNs) is able to compress eyes-closed resting electroencephalographic (EEG) data into spatial invariants of the instant voltage distributions for an automatic classification of mild cognitive impairment (MCI) and Alzheimer's disease (AD) subjects with classification accuracy of individual subjects higher than 92%.
Methods: Here we tested the hypothesis that this is the case also for the classification of individual normal elderly (Nold) vs. MCI subjects, an important issue for the screening of large populations at high risk of AD. Eyes-closed resting EEG data (10–20 electrode montage) were recorded in 171 Nold and in 115 amnesic MCI subjects. The data inputs for the classification by IFAST were the weights of the connections within a nonlinear auto-associative ANN trained to generate the instant voltage distributions of 60-s artifact-free EEG data.
Results: The most relevant features were selected and coincidently the dataset was split into two halves for the final binary classification (training and testing) performed by a supervised ANN. The classification of the individual Nold and MCI subjects reached 95.87% of sensitivity and 91.06% of specificity (93.46% of accuracy).
Conclusions: These results indicate that IFAST can reliably distinguish eyes-closed resting EEG in individual Nold and MCI subjects.
Significance: IFAST may be used for large-scale periodic screening of large populations at risk of AD and personalized care.

Keywords: Mild cognitive impairment (MCI); Alzheimer's disease (AD); Electroencephalography (EEG); Artificial neural networks (ANNs)

1. Introduction

The clinical condition called amnesic mild cognitive impairment (MCI) is characterized by objective evidence of memory impairment not yet encompassing the definition of dementia (Petersen et al., 1995, 2001). Amnesic MCI is

* Corresponding author. Address: Associazione Fatebenefratelli per la ricerca (AFaR), S. Giovanni Calibita- Isola Tiberina, 00185 Rome, Italy. Tel.: +39 06 6837300; fax: +39 06 49910917.
E-mail address: paolomaria.rossini@afar.it (P.M. Rossini).
URL: http://www.afar.it (P.M. Rossini).

1388-2457/$34.00
doi:10.1016/j.clinph.2008.03.026

considered as a precursor of Alzheimer's Disease (AD) (Scheltens et al., 2002) based on the high rate of progression from this state to the disease (Petersen et al., 2001). In normal aging, population annual conversion rate to AD ranges from 0.17% to 3.86% (Frisoni et al., 2004; Petersen et al., 2001). In MCI, that rate is remarkably higher ranging between 6 and 40% in the different series (Jack et al., 2005; Petersen et al., 2001). However, it should be remarked that a certain percentage of MCI subjects is not progressing into dementia at all (Jack et al., 1999; Petersen et al., 1995, 2001).

In order to plan optimal therapeutic, organizational, and rehabilitative interventions, it would be extremely important to make an early diagnosis of amnesic MCI in normal elderly subjects with the risk to develop AD. To this purpose, analysis of electroencephalographic (EEG) rhythms would be an ideal candidate, since it is a widely diffused, non-invasive, and low-cost procedure suitable for large-scale monitoring of large populations. In precedence, it has been shown that compared to normal elderly (Nold) subjects, AD patients presented excessive delta rhythms (0–3 Hz) and a significant decrement of posterior alpha rhythms (8–12 Hz; Babiloni et al., 2004; Dierks et al., 2000; Huang et al., 2000). Similarly, MCI subjects displayed a significant decrease of alpha power compared to Nold (Babiloni et al., 2006a,b,c; Koenig et al., 2005; Rossini et al., 2006). Furthermore, it has been reported a prominent decrease of functional coupling of EEG rhythms in AD and MCI when compared to Nold subjects (Adler et al., 2003; Babiloni et al., 2006a,b,c, 2007; Jelic et al., 2000; Prichep et al., 2006; Prichep, 2007; Rossini et al., 2006).

For fruitful clinical applications and personalized care, a crucial issue is the extent to which features of resting EEG data can be reliably used to distinguish individual Nold and amnesic MCI cases. Using global field power as an input (i.e. the sum of the EEG spectral power across all electrodes), it has been shown a discrimination and classification levels distinguishing between AD and MCI subjects of 84–78% (Bennys et al., 2001; Huang et al., 2000). Using the evaluation of spectral coherence between electrode pairs as an input (i.e. a measure of the EEG functional coupling), the correct classification between Nold and AD has reached an 82% level (Adler et al., 2003; Nuwer, 1997). The use of recurrent artificial neural networks (ANNs) to classify spectral EEG indexes has been able to discriminate AD and non-AD patients with a sensitivity of 80% and a specificity of 100% (Petrosian et al., 2001). In other studies, classifiers based on ANNs, wavelets, and blind source separation (BSS) have achieved promising results (Cichocki and Amari, 2003; Cichocki, 2004; Cichocki et al., 2005; Jeong, 2004; Vialette et al., 2005). The combination of them has classified resting EEG of MCI and AD subjects from 78.85% to 80.43% of accuracy (Buscema et al., 2007).

Topographic changes as well as modifications in the temporal fluctuation of the EEG voltage reflect loss of synaptic contacts as well as of cortico-cortical connections; meanwhile, cortical atrophy can affect the spatio-temporal pattern of neural synchronization generating the scalp EEG. These parameters have been used to successfully discriminate the respective distribution of probable Nold and AD subjects (Musha et al., 2002). The interesting new idea in that study (Musha et al., 2002) was the analysis of resting EEG voltage distribution instant by instant rather than the extraction of a global index along periods of tens of seconds or more. This idea has been further developed in a study on the zero-phase lag synchronization of EEG signals in aging, which has investigated the temporal relationships between EEG signals at paired recording sites (Koenig et al., 2005) as well as into a new procedure (implicit function as squashing time, IFAST) based on ANNs. The new procedure was able to compress eyes-closed resting EEG potential distributions into spatial invariants for an automatic classification of amnesic MCI and AD subjects with classification accuracy higher than 92% (Buscema et al., 2007). Here we tested the hypothesis that this is the case also for the classification of normal elderly (Nold) vs. MCI subjects, an important issue for the screening of large populations at risk of AD and personalized care. Eyes-closed resting EEG data were recorded in Nold and MCI subjects. The data inputs for the classification by IFAST were the weights of the connections within a non linear auto-associative ANN trained to generate the recorded data. The most relevant features were selected, and coincidently the dataset was split in two halves for the final binary classification (training and testing) performed by a supervised ANN.

2. Materials and methods

2.1. Subjects

This study was based on 171 Nold and 115 MCI subjects. Part of these individual datasets was used for parallel EEG studies in which we evaluated the power of EEG rhythms in pathological aging (Babiloni et al., 2006a,b,c, 2007; Rossini et al., 2006) or the automatic classification (IFAST) of resting EEG in MCI vs. AD subjects (Buscema et al., 2007).

Local institutional ethics committees approved the study. All experiments were performed with the informed and overt consent of each participant or caregiver, in line with the Code of Ethics of the World Medical Association (Declaration of Helsinki) and the standards established by the Author's Institutional Review Board.

The present inclusion and exclusion criteria for amnesic MCI were based on previous seminal studies (Albert et al., 1991; Devanand et al., 1997; Flicker et al., 1991; Petersen et al., 1995, 1997, 2001; Rubin et al., 1989; Portet et al., 2006; Zaudig, 1992) defining elderly persons, who do not meet the criteria for a diagnosis of dementia, with objective cognitive deficits, especially in the memory domain, as follows: (i) objective memory impairment on neuropsycholog-

ical evaluation, as defined by performances $\geqslant$1.5 standard deviation below the mean value of age and education-matched controls for a test battery including Busckhe–Fuld and Memory Rey tests; (ii) normal activities of daily living as documented by the history and evidence of independent living; and (iii) clinical dementia rating score of 0.5. The exclusion criteria for MCI included: (i) mild AD; (ii) evidence of concomitant dementia such as frontotemporal, vascular dementia, reversible dementias (including pseudo-depressive dementia), fluctuations in cognitive performance, and/or features of mixed dementias; (iii) evidence of concomitant extra-pyramidal symptoms; (iv) clinical and indirect evidence of depression as revealed by Geriatric Depression Scale scores higher than 13; (v) other psychiatric diseases, epilepsy, drug addiction, alcohol dependence, and use of psychoactive drugs including acetylcholinesterase inhibitors or other drugs enhancing brain cognitive functions; and (vi) current or previous uncontrolled or complicated systemic diseases (including diabetes mellitus) or traumatic brain injuries.

The Nold subjects were recruited mostly among non-consanguineous patients' relatives. All Nold subjects underwent physical and neurological examinations as well as cognitive screening. Subjects affected by chronic systemic illnesses, subjects receiving psychoactive drugs, and subjects with a history of present or previous neurological or psychiatric disease were excluded. All Nold subjects had a GDS score lower than 14 (no depression).

Table 1 summarizes the demographic and clinical data of Nold and MCI subjects.

2.2. EEG recordings

EEG data were recorded in the late morning in a fully awake, resting state (eyes-closed) from 19 electrodes positioned according to the International 10–20 System (i.e. Fp1, Fp2, F7, F3, Fz, F4, F8, T3, C3, Cz, C4, T4, T5, P3, Pz, P4, T6, O1, O2; 0.3–70 Hz bandpass; cephalic reference; see Fig. 1). To monitor eye movements, the horizontal and vertical electrooculogram (0.3–70 Hz bandpass) was also collected. All data were digitized in continuous recording mode (5 min of EEG; 128–256 Hz sampling rate). In order to keep constant the level of vigilance, an experimenter controlled on-line the subject and the EEG traces and alerted the subject any time there were signs of behavioral and/or EEG drowsiness.

Table 1
Demographic and neuropsychological data of healthy elderly (Nold) and mild cognitive impairment (MCI) subjects

	MCI	Nold
N	115	171
MMSE	25.2 (±0.2SE)	27.7 (±0.2SE)
Age	76.3 (±0.6SE)	64 (±1.4SE)
Education	8.2 (±0.4SE)	8.5 (±0.3SE)
IAF	8.9 (±0.1SE)	9 (±0.1SE)
Female/male	49M/66F	79M/92F

MMSE, mini mental state evaluation.

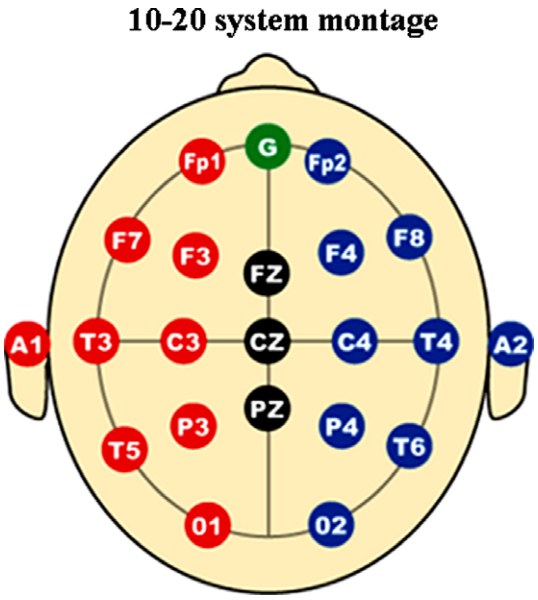

Fig. 1. Electroencephalographic (EEG) montage. EEG recordings were performed (0.3–70 Hz bandpass; cephalic reference) from 19 electrodes positioned according to the International 10–20 System.

Continuous EEG data were down-sampled to 128 Hz (EEG track). The EEG epochs with ocular, muscular, and other types of artifact were preliminarily identified by a computerized automatic procedure. EEG epochs with sporadic blinking artifacts (less than 10% of the total) were corrected by an autoregressive method (Moretti et al., 2003). Two independent experimenters blind to the diagnosis manually confirmed the EEG data accepted for further analysis.

2.3. Control spectral analysis of the EEG data

The statistical analysis of the EEG power density spectra between Nold and MCI subjects allowed the evaluation of the quality of the EEG data as an input for the IFAST analysis, with reference to the expected "slowing" of EEG rhythms in pathological aging, namely, lower alpha and a trend towards higher delta in the MCI than Nold subjects. A digital FFT-based power spectrum analysis (Welch technique, Hanning windowing function, no phase shift) computed power density of the EEG rhythms with 1 Hz frequency resolution. The following standard band frequencies were studied: delta (2–4 Hz), theta (4–8 Hz), alpha 1 (8–10 Hz), alpha 2 (10–12 Hz), beta 1 (13–20 Hz), beta 2 (20–30 Hz) and gamma (30-40 Hz). The spectral power density at each electrode was normalized to the spectral power density averaged across all frequencies (0.5-40 Hz) and across all electrodes.

The normalized spectral power density values were used as dependent variables for the ANOVA. The ANOVA factors (levels) were Group (Nold and MCI; independent var-

iable), Band (delta, theta, alpha 1, alpha 2, beta 1, beta 2, gamma), and Electrode (F3, Fz, F4, C3, Cz, C4, P3, Pz, P4, O1, O2). The Mauchly's test evaluated the sphericity assumption. Correction of the degrees of freedom was made with the Greenhouse–Geisser procedure. Age, gender, education, and individual alpha frequency (IAF; Klimesch, 1999) were used as covariates. The Tukey HSD test was used for post-hoc comparisons ($p < 0.05$).

2.4. IFAST (implicit function as squashing time)

Details on IFAST have been reported in a previous reference study (Buscema, 1999–2007, 2002, 2005–2007, 2007; Buscema et al., 2007). Briefly, the spatial content of the EEG voltage was extracted by IFAST step-wise procedure using ANNs. First, the data inputs for the classification operated by ANNs were not the EEG data, but the connections weights of a nonlinear auto-associative ANN trained to reproduce the recorded EEG tracks. These weights represented a good model of the peculiar spatial features of the EEG patterns at scalp surface. Second, the classification based on these parameters was binary (MCI vs. AD) and was performed by a supervised ANN. Half of the EEG database was used for the ANN training and the remaining half was utilised for the automatic classification phase (testing). More specifically, the IFAST method estimates implicit function from a multivariate data series (i.e. voltage EEG time series for several spatial locations) by compressing the temporal sequence of the EEG data into spatial invariants (i.e. the weights of auto-associated ANN nodes fitting the EEG data). The core of IFAST is that the ANNs do not classify subjects by directly using the EEG data as an input. Rather, the data inputs for the classification are the weights of the connections within a recirculation (non-supervised) ANN trained to generate the recorded EEG data. These connection weights represent a model of the peculiar spatial features of the EEG patterns at the scalp surface. The classification, based on these weights, is performed by a standard supervised ANN. In other words, the idea underlying the IFAST method resides in thinking that each patient's 19-channel EEG track can be synthesized by the connection parameters of an auto-associated nonlinear ANN trained on the same track's data.

There can be several topologies and learning algorithms for such ANNs; what is necessary is that the selected ANN is of the Auto-associated type (i.e. the input vector is the target for the output vector) and that the transfer functions defining it is nonlinear and differentiable at any point. Furthermore, it is required that all the processing made on every patient be carried out with the same type of ANN, and that the initial randomly generated weights have to be the same in every learning trial. This means that, for every EEG, every ANN has to have the same starting point, even if that starting point is random.

The phase of the IFAST is defined as "squashing", since it consists in compressing an EEG track in order to project on the connections of an auto-associated ANN the invariant patterns of that track. It is possible to use different types of auto-associated ANNs to run this search for spatial invariants in every EEG:

1. A back propagation without a hidden unit layer and without connections on the main diagonal (AutoBp). This is an ANN featuring an extremely simple learning algorithm. AutoBP works similarly to logistic regression and can be used to establish the dependency of variables from each other (for details see Buscema, 1998a; Rumelhart et al., 1986). The advantage of AutoBP is due to its learning speed, in turn due to the simplicity of its topology and algorithm. Moreover, at the end of the learning phase, the connections between variables, being direct, have a clear conceptual meaning. Every connection indicates a relationship of faded excitement, inhibition or indifference between every pair of channels in the EEG track of any patient. The disadvantage of AutoBP is its limited convergence capacity, due to that same topological simplicity. That is to say, complex relationships between variables may be approximated or ignored.
2. New recirculation network (NRC) is an original variation (Buscema, 1998b) of an ANN that has existed in the literature (Hinton and McClelland, 1988) and was not considered to be useful to the issue of auto-associating between variables. The topology of the NRC which we designed includes only one connection matrix and four layers of nodes: one input layer, corresponding to the number of variables; one output layer whose target is the input vector, and two layers of hidden nodes with the same cardinality independent from the cardinality of the input and output layers. The matrix between input-output nodes and hidden nodes is fully connected and in every learning cycle it is modified both ways. The advantages of NRC are its excellent convergence ability on complex datasets and, as a result, an excellent ability to interpolate complex relations between variables. The disadvantages mainly have to do with the vector codification that the hidden units run on the input vectors making difficult the conceptual decoding of its trained connections (Buscema, 1998a,b).
3. Auto-associative multi-layer perceptron (AMLP) may be used with an auto-associative purpose (encoding), thanks to its hidden units layer, that decomposes the input vector into main nonlinear components. The algorithm used to train the MLP is a typical back-propagation algorithm (Chauvin and Rumelhart, 1995). The MLP, with only one layer of hidden units, features two connection matrices and two intra-node connection vectors (bias). The advantages of MLP are its well-known flexibility and the strength of its back-propagation algorithm. Its disadvantages are the tendency to sat-

urate the hidden nodes when in the presence of non-stationary functions, and the vector codification (allocated) of the same hidden nodes (Chauvin and Rumelhart, 1995).

4. Elman's hidden recurrent (Elman, 1990) can be used for auto-associating purposes, again using the back-propagation algorithm (auto-associative hidden recurrent, AHR). It was used in our experimentation as a variation for MLP with memory set to one step. It is not possible to call it a proper recurring ANN in this form, because the memory would have been limited to one record before. We used this variation only to give the ANN an input vector modulated at any cycle by the values of the previous input vector. Our purpose was not to codify the temporal dependence of the entrance signals, but rather to give the ANN a "smoother" and more mediated input sequence. The number of connections in the AHR BP is the same as an MLP with extended input, whose cardinality is equal to the number of hidden units.

The entire sample of 286 subjects was recorded at 128 Hz for 1 min. IFAST classified Nold and MCI subjects based on 1-min of continuous artifact-free EEG data (EEG track). The EEG track for each subject was represented by a matrix of 7680 sequential rows (i.e. 128 Hz sampling rate $\times 60$ s) and 19 columns (i.e. 19 EEG electrodes of 10–20 montage system). Summarizing, the IFAST procedure was as follows:

1. The squashing phase of IFAST was implemented using the above four auto-associative ANNs with the topology reported in Table 2. Every auto-associative ANNs independently processed every EEG of the total sample in order to assess the different capabilities of each ANNs to extract the key information from the EEG tracks.
2. After this processing, each EEG track was squashed into the weights of every ANN, resulting in 4 different and independent datasets (one for each ANN), whose records were the squashing of the original EEG tracks and whose variables were the trained weights of every ANN.
3. The number of inputs (weights) of each record was, finally, compressed and selected by a special artificial organism able to understand the most relevant information present in all data (for the Input Selection Algorithm, I.S., see Buscema 2005–2007, Grossi and Buscema, 2006). After that, the 5×2 validation protocol for the independent identification of the spatial invariants of EEGs (Dietterich, 1988, Fig. 2) was applied blindly to test the capabilities of a generic supervised ANN to correctly classify each record. This is a robust protocol that allows one to evaluate the allocation of classification errors. In this procedure, the study sample is randomly divided ten times into two sub-samples, always different but containing a similar distribution of cases and controls. The ANN ability to classify all patients in the sample from the results of the confusion matrices (i.e. a confusion matrix describes the cardinalities of all pairwise intersections between two clustering results or partitions.) of these 10 independent experiments would indicate that the spatial invariants extracted and selected with our method truly relate to the functioning quality of the brains examined through their EEG.
4. A supervised MLP was used for the classification task, without hidden units. In every experimentation, in fact, we were able to train perfectly the ANN in no more than

Table 2
Auto-associative artificial neural networks (ANNs) types and parameters used during the processing

ANN parameters/type	ABp	NRC	AMLP	AHR
Number of inputs	19	19	19	19
Number of outputs	19	19	19	19
Number of state units	0	0	0	10
Number of hidden units	0	19	10	10
Number of weights	361	399	409	509
Number of epochs	200	200	200	200
Learning coefficient	0,1	0,1	0,1	0,1
Projection coefficient	Null	0,5	Null	Null

ABp, A back propagation without a hidden unit layer and without connections on the main diagonal; NRC, new recirculation network; AMLP, auto associative multi-layer perceptron; AHR, auto-associative hidden recurrent.

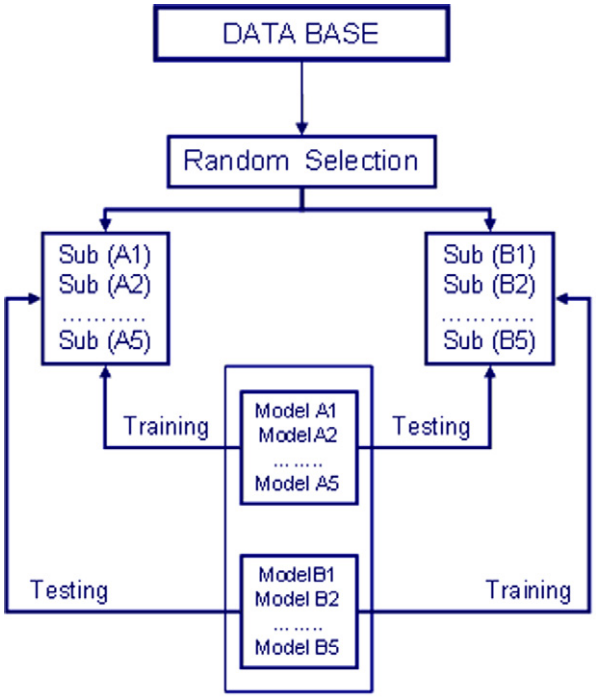

Fig. 2. 5×2 validation protocol for the independent identification of the spatial invariants of EEGs. *Legend:* Sub, Subject.

100 epochs (root mean square error (RMSE) <0.0001). That means that in this last phase, we could have used also a linear classifier to reach the same results.

The experimental design consisted in 10 different and independent processing for the classification Nold vs. MCI. Every experiment was conducted in a blind and independent manner in two directions: training with sub-sample A and blind testing with sub-sample B vs. training with sub-sample B and blind testing with sub-sample A.

3. Results

3.1. EEG power density spectrum

Fig. 3 illustrates the grand average of the normalized EEG spectral power density values computed in the Nold and MCI for the electrodes of interest (F3, Fz, F4, C3, Cz, C4, P3, Pz and P4) and for all frequency bands considered (delta, theta, alpha 1, alpha 2, beta 1, beta 2, gamma). As expected, the Nold subjects showed maximum power density values at alpha 1 band in the posterior regions; minimum values of EEG power density were detected at high frequency bands (beta 1, beta 2, and gamma). Compared to the Nold subjects, the amnesic MCI subjects showed a decrease of the posterior alpha power and an increase of frontal delta, theta and alpha power.

Statistical ANOVA of the EEG spectral power density values showed a significant interaction ($F(60,17040) = 17.4$; $p < 0.00001$) among the factors Group (Nold and MCI; independent variable), Band (delta, theta, alpha 1, alpha 2, beta 1, beta 2, gamma), and Electrode (F3, Fz, F4, C3, Cz, C4, P3, Pz, P4, O1, O2). Tukey HSD post-hoc testing showed that the normalized EEG spectral power density of alpha 1 and alpha 2 was stronger in amplitude in the Nold compared to the MCI subjects at P3, Pz, P4, O1 and O2 electrodes ($p < 0.00007$). On the contrary, the amplitude of normalized EEG spectral power density was lower in the Nold compared to MCI subjects at F3 (delta, theta and alpha 1 bands), Fz (alpha1 band), and F4 (delta and alpha1 bands) electrodes ($p < 0.002$).

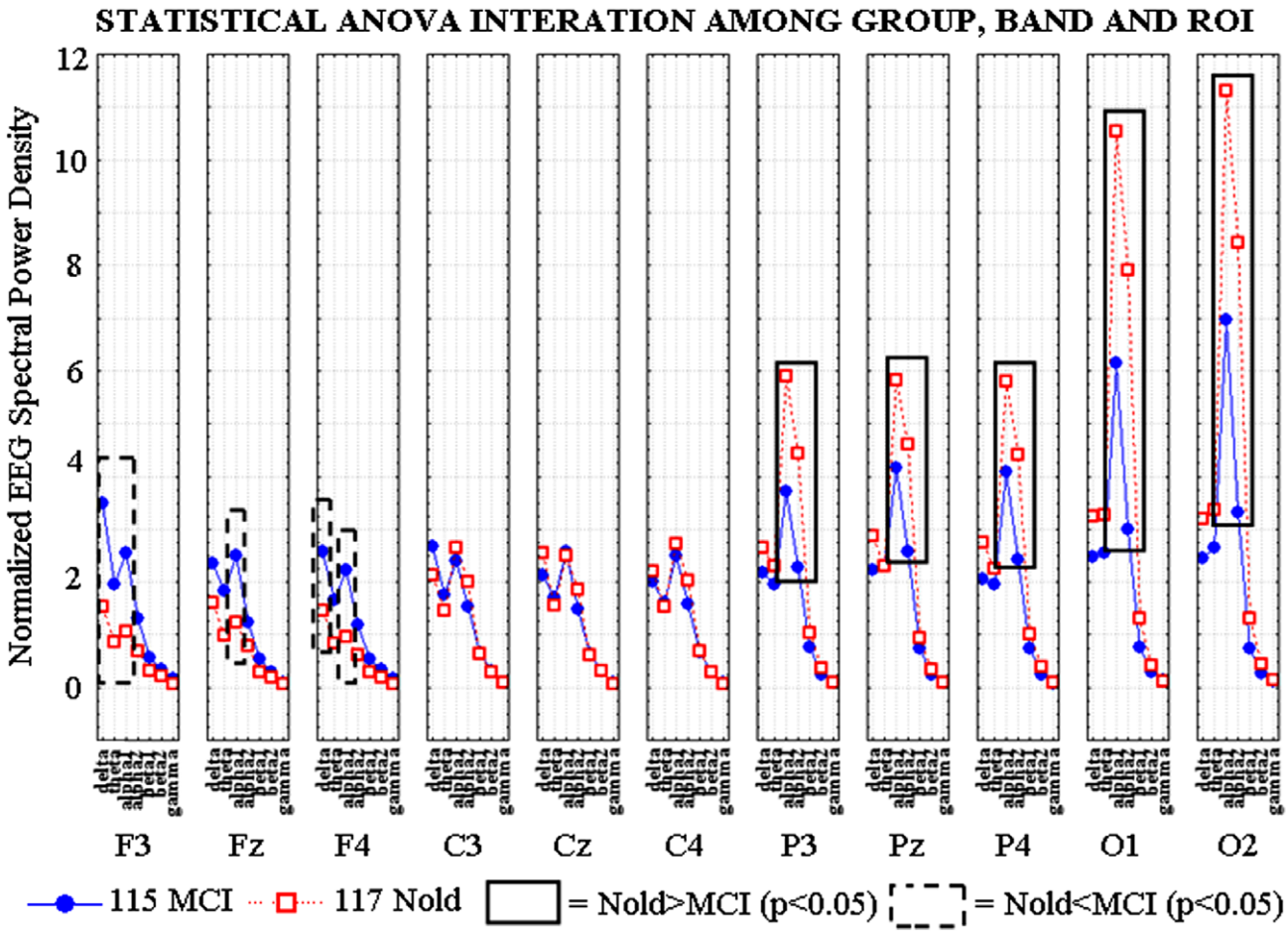

Fig. 3. Grand average of the EEG spectral power density values computed in the normal elderly (Nold) and mild cognitive impairment (MCI) subjects for the electrodes of interest (F3, Fz, F4, C3, Cz, C4, P3, Pz, P4, O1, O2) and for all frequency bands considered (delta, theta, alpha 1, alpha 2, beta 1, beta 2, gamma). The rectangles indicate the cortical regions and frequency bands in which the EEG spectral power density presented statistically significant different values with respect to the following patterns: Nold > MCI > , and Nold < MCI ($p < 0.05$, planned Duncan post hoc testing).

Table 3
Classification results of the four different auto-associated artificial neural networks (ANNs) in IFAST

Auto associated network type	SE (%)	SP (%)	Average mean accuracy (%)	Weighted mean accuracy (%)	Errors
AHR	96.16	85.82	90.99	89.98	14
NRC	96.30	92.17	92.73	92.87	10
AutoBp	93.09	91.39	92.24	92.07	11
AMLP	95.87	91.06	93.46	92.82	10

ABp, A back propagation without a hidden unit layer and without connections on the main diagonal; NRC, new recirculation network; AMLP, auto associative multi-layer perceptron; AHR, auto associative hidden recurrent; SE, sensibility; SP, specificity.

3.2. Automatic classification of Nold and MCI by IFAST

Table 3 reports the mean results for the classifications between Nold vs. MCI performed by the four different auto-associated networks in IFAST. It was noted that the ANN AMPL achieved the best results discriminating Nold vs. MCI subjects with 95.87% of sensitivity, 91.06% of specificity, and 93.46% of accuracy. The Table 4a and b report the details of the results obtained by the two best auto-associated ANNs (NRC and AMLP). Fig. 4a and b shows the corresponding average ROC curves.

3.3. Control analysis

Here IFAST procedure successfully classified individual Nold and MCI subjects based on resting voltage EEG data. (for theoretical considerations about how to use ANNs for individual classification in order to generate a statistics of each record (subject), see Grossi and Buscema, 2006). Additional information might be obtained by the evaluation of the classification values obtained by the different types of ANNs used within the general IFAST procedure. In the present control analysis, we used 10 different ANNs (see Table 5 for further details on the ANNs) for the binary classification (Nold vs. MCI) of each subject of the present database, namely, 115 MCI and 163 Nold subjects. Each ANN gave a classification value from 0 to 1, where the values from 0 to 0.5 corresponded to the classification as Nold and the values from 0.51 to 1 to the classification as MCI. The classification values were averaged for the 10 ANNs, in order to obtain the mean classification value for each subject. This value can be used to estimate the probability of correct classification for that subject. For example, one might arbitrarily define four levels of probability for the classification as Nold (classification score from 0 to 0.1, from 0.11 to 0.20, from 0.21 to 0.3, from 0.31 to 0.5), and four levels of probability for the classification as MCI (classification score from 0.9 to 1, from 0.8 to 0.89, from 0.7 to 0.79, and from 0.51 to 0.69). Each level of probability might be associated with a peculiar program of personalized monitoring. The above levels of probability also provide a further characterization of the present Nold and MCI groups. On the whole, 69.57% of the present MCI subjects reached the highest level of probability of correct classification, namely, from 0.9 to 1. Furthermore, 79.75% of the present Nold subjects reached the highest level of probability of correct classification, namely, from 0 to 0.1. Further details on the results of the control analysis are reported in Table 6.

4. Discussion

An ideal advancement in the challenge against AD would be the development of a non-invasive, objective and reliable, easy-to-perform, and low-cost diagnostic tool capable of contributing to an early diagnosis of amnesic MCI from a large at risk population sample, namely, subjects with genetic defects or a family history

Table 4
Details of the two best artificial neural networks (ANNs) used for the present study results

ANN	Nold	MCI	SE	SP	A.M.Acc.	W.M.Acc.	VP	VN	FP	FN	VP+	VP−	LR+	LR−	AUC
(a) NRC results details															
FF_Bp(ab)	74	85	94.6	90.6	92.59	92.45	70	77	8	4	89.7	95.1	10.1	0.06	~0.929
FF_Bp(ba)	41	78	100	89.7	94.87	93.28	41	70	8	0	83.7	100	9.75	0	~0.939
Mean			97.3	90.2	93.73	92.87	56	74	8	2	86.7	97.5	9.9	0.03	~0.94
(b) AMLP results details															
TasmSABp(ab)	52	98	98.1	89.8	93.94	92.67	51	88	10	1	83.6	98.9	9.61	0.02	~0.928
TasmSABp(ba)	63	65	93.7	92.3	92.98	92.97	59	60	5	4	92.2	93.8	12.2	0.07	~0.916
Mean			95.9	91.1	93.46	92.82	55	74	8	2.5	87.9	96.3	10.9	0.05	0.92

NRC, new recirculation network; AMLP, auto-associative multi-layer perceptron; MCI N., number of subject in the MCI sample of testing file; Nold N., number of subjects in the Nold sample of testing file; SE, sensibility; SP, specificity; A.M.Acc., average mean accuracy; W.M.Acc., weighted mean accuracy; VP, positive value; VN, negative value; FP, false positive; FN, false negative; VP+, positive predictive value; VP−, negative predictive value; LR+, likelihood ratio for a positive test results (benchmark value $\geqslant 2$); LR−, likelihood ratio for a negative test results (benchmark value $\leqslant 0.2$); AUC, area under ROC curve (average ROC curve calculated by the threshold method).

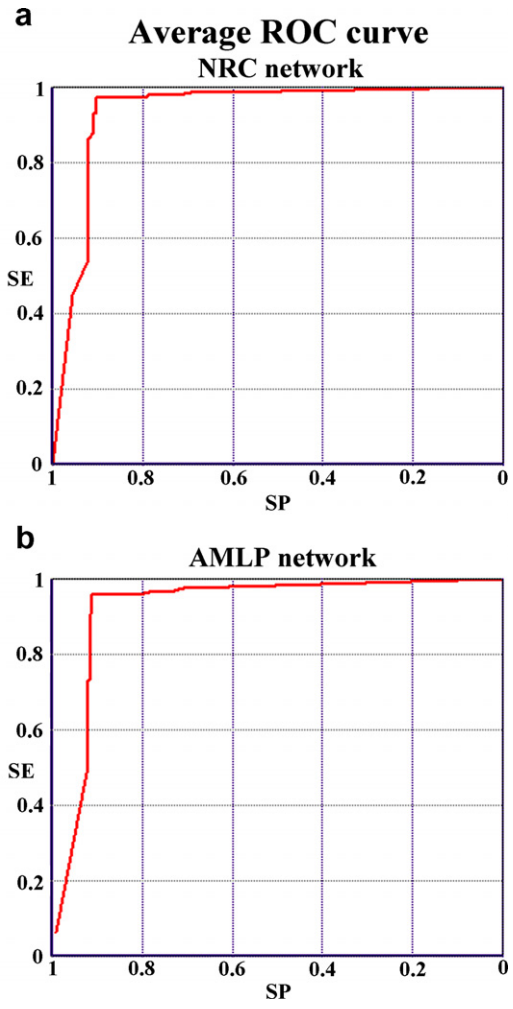

Fig. 4. (a) Average ROC curve illustrating the results of NRC network used for the present study (AUC ~0.94); (b) Average ROC curve illustrating the results of the AMLP network used for the present study (AUC ~0.92). NRC, new recirculation network; AUC, area under ROC curve (Average ROC curve calculated by the threshold method); AMLP, auto-associative multi-layer perceptron; SE, sensibility; SP, specificity.

of dementias. Here we tested the hypothesis that an ANN procedure called IFAST is able to automatically classify Nold and amnesic MCI individuals based on the topography of 1-min, eyes-closed, artifact-free resting EEG voltage.

As a preliminary control analysis, we compared the eyes-closed resting EEG power in the recruited Nold and amnesic MCI subjects. When compared to the Nold subjects, the amnesic MCI subjects showed a lower power of alpha rhythms in line with previous evidence on pathological brain aging (Babiloni et al., 2006a,b,c, 2007; Dierks et al., 1993, 2000; Koenig et al., 2005; Rodriguez et al., 1999a,b; Rossini et al., 2006). From a methodological viewpoint, the results of this preliminary analysis validated our general procedures for subjects' recruitment and EEG data selection.

Concerning the performance by IFAST on the topography of EEG voltage, the results showed that the individual Nold and amnesic MCI subjects were classified with 91–93% of accuracy. These results suggest that the IFAST successfully compressed eyes-closed resting EEG data into spatial invariants (i.e. global and stable features characterizing a family of individual cases) of the instant voltage distributions for an effective automatic classification of Nold and amnesic MCI individuals. In this sense, the results complement the previous evidence showing that IFAST was able to classify amnesic MCI vs. AD subjects with about 92% of accuracy (Buscema et al., 2007).

In the present study, the highest classification rate between Nold and amnesic MCI subjects was reached by an AMLP (auto-associative multi-layer perceptron) with only one layer of hidden units, two connection matrices, and two intra-node connection vectors as bias (Chauvin and Rumelhart, 1995). The strength of MLP stems into the flexibility of back-propagation algorithm, which compensates its tendency to saturate the hidden nodes in the presence of non-stationary functions (Chauvin and Rumelhart, 1995). The present results are in agreement with a reference IFAST study (Buscema et al., 2007) in which MPL and its variant called AHR (auto-associative hidden recurrent; Elman, 1990) have automatically classified the topography of EEG voltage in amnesic MCI vs. AD subjects with 91–92% of accuracy.

Given the results, a main issue is "Why is IFAST so effective in the EEG classification of Nold and MCI subjects?" IFAST represents spatial invariance of the eyes-closed, 60-s, artifact-free resting EEG voltages as the weights of an auto-associative ANN having an input and output node for each scalp electrode. For each subject, these weights indicate the strength of the reciprocal connections between the nodes of the ANN, which explains the topography of the EEG voltages recorded in that subject. Therefore, the ANN weights can be considered as a rough but effective model of the brain "default" networks generating eyes-closed resting EEG data, which might reflect ongoing and costly intrinsic activity within brain systems that most likely represents the largest fraction of the brain's background activity (Raichle and Gusnard, 2005; Raichle and Mintun, 2006). It can be speculated that the success of IFAST relies into the classification of Nold and MCI subjects based on the ANN weights explaining eyes-closed resting EEG data, which would be less variable and noise-dependent than the explained EEG voltage itself. Use of EEG spectral indexes has allowed classifications between Nold and AD or between MCI and AD subjects with less than 90% of accuracy. Specifically, summing EEG spectral power across all electrodes allowed classifications between AD and MCI subjects with 84–78% of accuracy (Huang et al., 2000; Bennys et al., 2001). The use of EEG spectral coherence between electrodes resulted in classifications between Nold and AD subjects with 82% of accuracy (Adler et al., 2003; Nuwer, 1997), whereas other EEG spectral indexes determined classifications between Nold vs. AD or MCI vs. AD subjects with 80–85% of accuracy (Buscema et al., 2007; Cichocki and Amari, 2003; Cichocki,

Table 5
The ten different ANNs used for the binary classification (Nold vs. MCI) of each subject of the present database in a control analysis

n	ANN	SE	SP	A.M.Acc.	W.M.Acc.	VP	VN	FP	FN	VP+	VP−	RV+	RV−	AUC
1	FF_Bm(ab)	98.1	87	92.41	90.67	51	85	13	1	79.7	98.84	7.39	0.02	0.941
	FF_Bm(ba)	93.7	92	92.98	92.97	59	60	5	4	92.2	93.75	12.2	0.07	0.953
2	FF_Bp(ab)	98.1	87	92.41	90.67	51	85	13	1	79.7	98.84	7.39	0.02	0.938
	FF_Bp(ba)	93.7	92	92.98	92.97	59	60	5	4	92.2	93.75	12.2	0.07	0.913
3	SelfDABm(ab)	98.1	86	91.9	90	51	84	14	1	78.5	98.82	6.87	0.02	0.934
	SelfDABm(ba)	95.2	91	93	92.97	60	59	6	3	90.9	95.16	10.3	0.05	0.921
4	SelfDABp(ab)	100	86	92.86	90.67	52	84	14	0	78.8	100	7	0	0.92
	SelfDABp(ba)	93.7	92	92.98	92.97	59	60	5	4	92.2	93.75	12.2	0.07	0.932
5	SelfSABm(ab)	94.2	91	92.52	92	49	89	9	3	84.5	96.74	10.3	0.06	0.908
	SelfSABm(ba)	90.5	95	92.93	92.97	57	62	3	6	95	91.18	19.6	0.1	0.932
6	SelfSABp(ab)	98.1	88	92.92	91.33	51	86	12	1	81	98.85	8.01	0.02	0.93
	SelfSABp(ba)	93.7	92	92.98	92.97	59	60	5	4	92.2	93.75	12.2	0.07	0.934
7	TasmDABm(ab)	100	85	92.35	90	52	83	15	0	77.6	100	6.53	0	0.923
	TasmDABm(ba)	95.2	91	93	92.97	60	59	6	3	90.9	95.16	10.3	0.05	0.926
8	TasmDABp(ab)	98.1	87	92.41	90.67	51	85	13	1	79.7	98.84	7.39	0.02	0.936
	TasmDABp(ba)	93.7	92	92.98	92.97	59	60	5	4	92.2	93.75	12.2	0.07	0.935
9	TasmSABm(ab)	98.1	87	92.41	90.67	51	85	13	1	79.7	98.84	7.39	0.02	0.925
	TasmSABm(ba)	95.2	91	93	92.97	60	59	6	3	90.9	95.16	10.3	0.05	0.95
10	TasmSABp(ab)	98.1	90	93.94	92.67	51	88	10	1	83.6	98.88	9.61	0.02	0.928
	TasmSABp(ba)	93.7	92	92.98	92.97	59	60	5	4	92.2	93.75	12.2	0.07	0.916
	Mean	93.8	92	92.98	92.97	59.1	59.9	5.1	3.9	92.1	93.92	12.4	0.07	0.93

FF, Feed Forward networks; FF_Bm, feed forward network with BiModal learning law (BiModal network was developed at Semeion Center, Buscema 2003); FF_Bp, Feed Forward network with back-propagation learning law; Self, self recurrent networks (created at Semeion Center; Buscema, 1995, Buscema et al., 2006), which are composed in a feedback loop, by a normal Feed Forward network, an auto-associative Feed Forward network with two layers and an additional layer of (PEs), called extended input. The auto-associative network receives in input, the feedback signal in input from PEs of the feed forward of the hidden layer, through mono-dedicated connections. Outputs from PEs of the output layer of the auto-associative are connected, through mono-dedicated connections, to correspondent PEs of the extended input layer. Finally, outputs from PEs of the extended input layer are distributed in input to PEs of the Feed Forward hidden layer, through complete net connections. The patterns processed by the auto-associative coincide with the outputs of the hidden layer of the Feed Forward; SelfSA, self recurrent network, static version; the SelfDA is the dynamic version, introducing a dependence of the activation functions of the Feed Forward hidden layer on the weights of the connections of the auto-associative. This dependence should increase feedback dynamism of this architecture; SelfSABp, self recurrent network, static version, with back-propagation learning algorithm; SelfSABm, self recurrent network, static version, with BiModal learning algorithm; SelfDABp, self recurrent network, dynamic version, with back-propagation learning algorithm; SelfDABm, self recurrent network, dynamic version, with BiModal learning algorithm; TASM, temporal associative subjective memory, which is constituted, topologically, by a composition, in a feedback loop, of a normal Feed Forward network, SelfReflexive (SR) network with free hidden units, which is a drift model with an additional layer of PEs, called extended input. SR network receives in input the feedback signal from PEs of the hidden layer of the Feed Forward, through mono-dedicated connections. Outputs from PEs of the free hidden layer of the SelfReflexive are connected, through mono-dedicated connections, to correspondent PEs of the extended input layer. Finally, outputs from PEs of the extended input layer are distributed in input, to PEs of the Feed Forward hidden layer, through full grid connections. Inner connections of Feed Forward and SelfReflexive networks, as well as those connecting the extended input layer to the Feed Forward hidden layer, have an adaptive weight. Connections linking the Feed Forward hidden layer to the SelfReflexive input layer, and those linking the SelfReflexive free hidden layer to the extended input layer have a fixed weight, equal to 1, since they have their only function of is to copy or "clone" the activation value. In a TASM network (n+1)-th, input model is not accompanied with simple "traces" that the network had carried out on the previous n-th model, but rather with a synthetic elaboration (clustering) of the memory of the previous model. SelfReflexive free units supply the values for what we could define a metamemory; TASMDa = dynamic Tasm network, which is a modification of the static version of TASM networks. It consists in introducing in the activation functions of the Feed Forward hidden layer a dependence of the weights of the input-hidden connection on the activation values of the extended input. This dependence corresponds to the introduction of a node-connection meta-arch, namely, a connection to each input-hidden weight so that the *j*-th PE of the hidden layer is the product of the activation values of all PEs of the extended input; TasmSABp, TASM recurrent network, static version, with back-propagation learning algorithm; TasmSABm, TASM recurrent network, static version, with BiModal learning algorithm; TasmDABp, TASM recurrent network, dynamic version, with back-propagation learning algorithm; TasmDABm, TASM recurrent network, dynamic version, with BiModal learning algorithm.

2004; Cichocki et al., 2005; Jeong, 2004; Petrosian et al., 2001; Vialette et al., 2005).

At the present stage of research, the relationships between abnormal topography of eyes-closed resting EEG voltage and AD processes can be only hypothesized. An important but not exclusive role might be played by a lack of the excitatory neurotransmitter acetylcholine into cholinergic neural projections from basal forebrain to hippocampus/amygdala and cortex reported in previous post-mortem AD studies (Francis et al., 1999; Mesulam, 2004). This explanation is supported by several lines of evidence. The residual integrity of cholinergic systems is related to the effects of cholinester-

Table 6
Mean classification values resulting from the use of 10 ANNs on the EEG data of each Nold and MCI subject

	% of subjects	Number of subjects
Clinical diagnosis of MCI		
0.9–1	69.57	80
0.8–0.89	15.65	18
0.7–0.79	9.57	11
0.51–0.69	3.48	4
Equal or lower than 0.5 (=Nold)	2.61	3
Clinical diagnosis of Nold		
0–0.1	79.75	130
0.11–0.20	1.84	3
0.21–0.3	3.68	6
0.31–0.5	5.52	9
Higher than 0.5 (=MCI)	9.20	15

Each ANN gave a classification value from 0 to 1, where the values from 0 to 0.5 corresponded to the classification as Nold and the values from 0.51 to 1 to the classification as MCI. The mean classification value can be used to estimate the probability of correct classification for that subject. The distribution of the present Nold and MCI subjects was provided for several ranges of the classification values.

ase inhibitors in AD (Tanaka et al., 2003). Abnormal EEG activity similar to the one encountered in AD can be induced in healthy subjects by transient use of a cholinergic synaptic blocker like scopolamine (Kikuchi et al., 2000; Villa et al., 2000). Long-term (1 year) treatment of acetylcholinesterase inhibitors produces clear effects on the resting EEG activity in responders when compared to non-responders (Babiloni et al., 2006d; Rodriguez et al., 2002). However, it should be remarked that the relationships between cholinergic tone and neurodegenerative processes in AD patients may be nonlinear. Indeed, two studies have suggested that cognitive deficits in MCI and early AD subjects were not associated with the loss of cholinergic levels (Davis et al., 1999; DeKosky et al., 2002). In the first study (Davis et al., 1999), neocortical cholinergic deficits were characteristic of severely demented AD patients, but cholinergic deficits were not apparent in individuals with mild AD. In the second study (DeKosky et al., 2002), the cholinergic system determined compensatory responses during the early stage of dementia (DeKosky et al., 2002). This up-regulation was seen in frontal cortex and could be an important factor in preventing the transition of MCI subjects to AD (DeKosky et al., 2002). Furthermore, it should be remarked that abnormal EEG rhythms can be observed not only in people with pathological aging but also in other kinds of neurologic disorders not clearly related to an impairment of cholinergic systems (Priori et al., 2004). Finally, brain arousal and corresponding EEG oscillations would depend on a complex balance among neurotransmitters systems; together with cholinergic systems, monoaminergic (Dringenberg, 2000) and non-NMDA vs. NMDS glutamatergic unbalance (Di Lazzaro et al., 2004) might affect cortical excitability and EEG rhythms in AD patients as well. On the whole, "cholinergic" explanation of abnormal EEG changes in MCI and AD patients is an interesting theoretical option but needs conclusive "in vivo" empirical support.

A crucial issue of the present study is "May IFAST contribute to an early instrumental diagnosis of MCI in large elderly populations?" Non-reversible forms of dementias represent a major health problem in all those countries where the average life-span is progressively increasing. An early clinical and diagnostic evidence of AD is prevented by the fact that for a long-lasting pre-clinical stage brain neural networks rearrange via plasticity mechanisms their connections and synapses to compensate neural loss due to neuro-degeneration (Babiloni et al., 2000; Ferreri et al., 2003; Stern, 2006). This process of plasticity maintains cognitive functions for years before clinical symptoms of dementia appear, especially in the case that high education and large brain size (i.e. brain reserve) mask underlying disease pathology (Mortimer et al., 2005). Optimum instrumental approaches for early diagnosis of pre-clinical AD stages like MCI therefore need to target the severity of underlying brain pathology independently of brain reserve. This criterion seems to be satisfied by IFAST using just 60-s eyes-closed resting EEG data as an input. Indeed, IFAST was able to classify not only MCI vs. AD (Buscema et al., 2007) but also Nold vs. MCI with accuracy higher than 90%. However, even if confirmed in control longitudinal studies, this rate is clearly insufficient for the use of IFAST procedure alone for a definite diagnosis of MCI. In the case of IFAST positive alarm, further neuropsychological and instrumental approaches should be used to ascertain the presence of MCI status.

The present results prompt prospective studies on the predictive value of IFAST in the prediction of the conversion to MCI to AD or back to normalcy. However, apart of clinical perspectives, the present findings have an intrinsic value for clinical neurophysiology. They provided further functional data from a large aged population to support the idea that spatial features of eyes-closed resting EEG, as a reflection of the cortical neural synchronization, convey information content able to discriminate pre-clinical stage of dementia (amnesic MCI) from Nold when a sophisticated mathematical approach based on ANNs is available.

5. Conclusions

We tested the hypothesis that a new procedure (implicit function as squashing time, IFAST) based on ANNs is able to compress eyes-closed resting EEG data into spatial invariants of the instant voltage distributions for a reliable automatic classification of Nold and amnesic MCI subjects, an important issue for the screening of large populations at risk of AD. The data inputs for the classification by IFAST were the weights of the connections within a non-linear auto-associative ANN trained to generate the recorded EEG data. The classification of the Nold and MCI subjects reached 95.87% of sensitivity, 91.06% of specificity, and 93.46% of accuracy. The results indicate that IFAST can reliably distinguish eyes-closed resting EEG in Nold and amnesic MCI subjects, and may be used

for large-scale periodic screening in population at risk of AD (after confirmation on independent large populations of Nold and MCI subjects). This is a clearly new information provided by the IFAST procedure in the attempt to discriminate individual EEG data in that clinical shadow context separating normalcy from initial cognitive impairment, a condition of especial interest for an early diagnosis of MCI. In this sense, the present study represents a step forward with respect to a previous successful application of the IFAST procedure for the classification of individual MCI and AD subjects, which was theoretically facilitated by the strong EEG changes associated with dementia processes (Buscema et al., 2007).

Acknowledgments

The research was granted by the Association Fatebenefratelli for Research (AFaR), BIOPATTERN PROJECT and SEMEION. We thank Prof. Fabrizio Eusebi for his continuous support.

References

Adler G, Brassen S, Jajcevic A. EEG coherence in Alzheimer's dementia. J Neural Transm 2003;110:1051–8.

Albert M, Smith LA, Scherr PA, Taylor JO, Evans DA, Funkenstein HH. Use of brief cognitive tests to identify individuals in the community with clinically diagnosed Alzheimer's disease. Int J Neurosci 1991;57(3–4):167–78.

Babiloni C, Babiloni F, Carducci F, Cincotti F, De Pino G, Del Percio C, et al. Movement-related in electroencephalographic reactivity in Alzheimer disease. NeuroImage 2000;12(2):139–46.

Babiloni C, Binetti G, Cassetta E, Cerboneschi D, Dal Forno G, Del Percio C, et al. Mapping distributed sources of cortical rhythms in mild Alzheimers disease. A multi-centric EEG study. NeuroImage 2004;22(1):57–67.

Babiloni C, Binetti G, Cassetta E, Dal Forno G, Del Percio C, Ferreri F, et al. Sources of cortical rhythms change as a function of cognitive impairment in pathological aging: a multi-centric study. Clin Neurophysiol 2006a;117(2):252–68.

Babiloni C, Benussi L, Binetti G, Bosco P, Busonero G, Cesaretti S, et al. Genotype (cystatin C) and EEG phenotype in Alzheimer disease and mild cognitive impairment: a multicentric study. Neuroimage 2006b;29(3):948–64.

Babiloni C, Benussi L, Binetti G, Cassetta E, Dal Forno G, Del Percio C, et al. Apolipoprotein E and alpha brain rhythms in mild cognitive impairment: a multicentric EEG study. Ann Neurol 2006c;59(2):323–34.

Babiloni C, Cassetta E, Dal Forno G, Del Percio C, Ferreri F, Ferri R, et al. Donepezil effects on sources of cortical rhythms in mild Alzheimer's disease: responders vs. non-responders. Neuroimage 2006d;31(4):1650–65.

Babiloni C, Squitti R, Del Percio C, Cassetta E, Ventriglia MC, Ferreri F, et al. Free copper and resting temporal EEG rhythms correlate across healthy, mild cognitive impairment, and Alzheimer's disease subjects. Clin Neurophysiol 2007;118:1244–60.

Bennys K, Rondouin G, Vergnes C, Touchon J. Diagnostic value of quantitative EEG in Alzheimer disease. Neurophysiol Clin 2001;31(3):153–60.

Buscema M. Constraint satisfaction neural networks. In: Buscema M, editor. Substance use and misuse. Special issue on artificial neural networks and complex social systems. Marcel Dekker; New York: 1998a;33(2):389–408.

Buscema M. Bi Modal Networks Technical Paper n. 29, 2003.

Buscema M. Self-Reflexive Networks. Theory, Topology, Applications, in Quality & Quantity, Kluver Academic Publishers, The Netherlands, Vol. 29, n. 4, November 1995, pp. 339–403.

Buscema M, Breda M, Terzi S. New Recurrent Neural Architectures, Proceedings of the 2006 WSEAS International Conference on Mathematical Biology and Ecology, Miami, Florida, USA, January 18–20, 2006, pp. 174–201.

Buscema M. Recirculation neural networks. In: M. Buscema, editor. Substance use and misuse. Special issue on artificial neural networks and complex social systems. Marcel Dekker; New York: 1998b;33(2):383–88.

Buscema M, Rossini P, Babiloni C, Grossi E. The I.F.A.S.T. Model, a novel parallel non-linear EEG analysis technique, distinguishes mild cognitive impairment and Alzheimer's disease patients with high degree of accuracy. Artif Intel Med 2007;40(2):127–41.

Buscema M. I FAST Software, ver 7.0, Semeion Software #32, Rome, Italy, 2005–2007.

Buscema M. Supervised ANNs and organisms, ver 12.5, Semeion Software # 12, Rome, Italy, 1999–2007.

Buscema M. Input Search (I.S.), ver 2.0, Semeion Software #17, Rome, Italy, 2002.

Buscema M. Twist: input search and T& T reverse, ver 2.0, Semeion Software #39, Rome, Italy, 2007.

Chauvin Y, Rumelhart DE. Back propagation: theory, architectures, and applications. New Jersey: Lawrence Erlbaum Associates, Inc. Publishers 365 Brodway- Hillsdale; 1995.

Cichocki A, Amari S. Adaptive blind signal and image processing: learning algorithms and applications. New York, NY: Wiley; 2003.

Cichocki A. Blind signal processing methods for analyzing multichannel brain signals. Int J Bioelectromagnetism 2004;6(1).

Cichocki A, Shishkin S, Musha T, Leonowicz Z, Asada T, Kurachi T. EEG Filtering based on blind source separation (BSS) for early detection of Alzheimer's disease. Clin Neurophysiol 2005;116(3):729–37.

Davis KL, Mohs RC, Marin D, Purohit DP, Perl DP, Lantz M, et al. Cholinergic markers in elderly patients with early signs of Alzheimer disease. JAMA 1999;281(15):1401–6.

Devanand DP, Folz M, Gorlyn M, Moeller JR, Stern Y. Questionable dementia: clinical course and predictors of outcome. J Am Geriatr Soc 1997;45(3):321–8.

DeKosky ST, Ikonomovic MD, Styren SD, Beckett L, Wisniewski S, Bennett DA, et al. Upregulation of choline acetyltransferase activity in hippocampus and frontal cortex of elderly subjects with mild cognitive impairment. Ann Neurol 2002;51(2):145–55.

Dierks T, Ihl R, Frolich L, Maurer K. Dementia of the Alzheimer type: effects on the spontaneous EEG described by dipole sources. Psychiatry Res 1993;50(3):151–62.

Dierks T, Jelic V, Pascual-Marqui RD, Wahlund L, Julin P, Linden DE, et al. Spatial pattern of cerebral glucose metabolism (PET) correlates with localization of intracerebral EEG-generators in Alzheimer's disease. Clin Neurophysiol 2000;111(10):1817–24.

Dietterich TG. Approximate statistical tests for comparing supervised classification learning algorithms. Neural Comput 1988;10(7):1895–924.

Di Lazzaro V, Oliviero A, Pilato F, Saturno E, Dileone M, Marra C, et al. Motor cortex hyperexcitability to transcranial magnetic stimulation in Alzheimer's disease. J Neurol Neurosurg Psychiatry 2004;75:555–9.

Dringenberg HC. Alzheimer's disease: more than a'cholinergic disorder' – evidence that cholinergic-monoaminergic interactions contribute to EEG slowing and dementia. Behav Brain Res 2000;115:235–49.

Elman JL. Finding structure in time. Cognitive Sci 1990;14:179–211.

Ferreri F, Pauri F, Pasqualetti P, Fini R, Dal Forno G, Rossini PM. Motor cortex excitability in Alzheimer's disease: a transcranial magnetic stimulation study. Ann Neurol 2003;53(1):102–8.

Flicker C, Ferris SH, Reisberg B. Mild cognitive impairment in the elderly: predictors of dementia. Neurology 1991;41(7):1006–9.

Francis PT, Palmer AM, Snape M, Wilcock GK. The cholinergic hypothesis of Alzheimer's disease: a review of progress. J Neurol Neurosurg Psychiatry 1999;66(2):137–47.

Frisoni GB, Padovani A, Wahlund LO. The predementia diagnosis of Alzheimer disease. Alzheimer Dis Assoc Disord 2004;18(2):51–3.

Grossi E, Buscema M. Artificial intelligence and outcome research. Drug Dev Res 2006;67:227–44.

Hinton GE, McClelland JL. Learning representation by recirculation. In: Proceeding of IEEE conference on neural information processing systems. Denver, Colo, USA, 1988.

Huang C, Wahlund L, Dierks T, Julin P, Winblad B, Jelic V. Discrimination of Alzheimer's disease and mild cognitive impairment by equivalent EEG sources: a cross-sectional and longitudinal study. Clin Neurophysiol 2000;111(11):1961–7.

Jack Jr CR, Petersen RC, Xu YC, O'Brien PC, Smith GE, Ivnik RJ, et al. Prediction of AD with MRI-based hippocampal volume in mild cognitive impairment. Neurology 1999;52(7):1397–403.

Jack Jr CR, Shiung MM, Weigand SD, O'Brien PC, Gunter JL, Boeve BF, et al. Brain atrophy rates predict subsequent clinical conversion in normal elderly and amnestic MCI. Neurology 2005;65(8):1227–31.

Jelic V, Johansson SE, Almkvist O, Shigeta M, Julin P, Nordberg A, et al. Quantitative electroencephalography in mild cognitive impairment: longitudinal changes and possible prediction of Alzheimer's disease. Neurobiol Aging 2000;21(4):533–40.

Jeong J. EEG dynamics in patients with Alzheimer's disease. Clin Neurophysiol 2004;115:1490–505.

Kikuchi M, Wada Y, Koshino Y, Nanbu Y, Hashimoto T. Effects of scopolamine on interhemispheric EEG coherence in healthy subjects: analysis during rest and photic stimulation. Clin Electroencephalogr 2000;31(2):109–15.

Klimesch W. EEG alpha and theta oscillations reflect cognitive and memory performance: a review and analysis. Brain Res Brain Res Rev 1999;29(2–3):169–95.

Koenig T, Prichep L, Dierks T, Hubl D, Wahlund LO, John ER, et al. Decreased EEG synchronization in Alzheimer's disease and mild cognitive impairment. Neurobiol Aging 2005;26(2):165–71.

Mesulam M. The cholinergic lesion of Alzheimer's disease: pivotal factor or side show? Learn Mem 2004;11(1):43–9.

Moretti DV, Babiloni F, Carducci F, Cincotti F, Remondini E, Rossini PM, et al. Computerized processing of EEG-EOG-EMG artefacts for multi-centric studies in EEG oscillations and event-related potentials. Int J Psychophysiol 2003;47(3):199–216.

Mortimer JA, Borenstein AR, Gosche KM, Snowdon DA. Very early detection of Alzheimer neuropathology and the role of brain reserve in modifying its clinical expression. J Geriatr Psychiatry Neurol 2005;18(4):218–23.

Musha T, Asada T, Yamashita F, Kinoshita T, Chen Z, Matsuda H, et al. A new EEG method for estimating cortical neuronal impairment that is sensitive to early stage Alzheimer's disease. Clin Neurophysiol 2002;113:1052–8.

Nuwer M. Assessment of digital EEG, quantitative EEG, and EEG brain mapping: report of the American Academy of Neurology and the American Clinical Neurophysiology Society. Neurology 1997;49(1): 277–92, Review.

Petersen RC, Smith GE, Ivnik RJ, Tangalos EG, Schaid SN, Thibodeau SN, et al. Apolipoprotein E status as a predictor of the development of Alzheimer's disease in memory-impaired individuals. JAMA 1995;273:1274–8.

Petersen RC, Smith GE, Waring SC, Ivnik RJ, Kokmen E, Tangelos EG. Aging, memory, and mild cognitive impairment. Int Psychogeriatr 1997;9(1):65–9.

Petersen RC, Doody R, Kurz A, Mohs RC, Morris JC, Rabins PV, et al. Current concepts in mild cognitive impairment. Arch Neurol 2001;58(12):1985–92.

Petrosian AA, Prokhorov DV, Lajara-Nanson W, Schiffer RB. Recurrent neural network-based approach for early recognition of Alzheimer disease in EEG. Clin Neurophysiol 2001;112:1378–87.

Prichep LS, John ER, Ferris SH, Rausch L, Fang Z, Cancro R, et al. Prediction of longitudinal cognitive decline in normal elderly with subjective complaints using electrophysiological imaging. Neurobiol Aging 2006;27:471–81.

Prichep LS. Quantitative EEG and electromagnetic brain imaging in aging and in the evolution of dementia. Ann NY Acad Sci 2007;1097:156–67.

Priori A, Foffani G, Pesenti A, Tamma F, Bianchi AM, Pellegrini M, et al. Rhythm-specific pharmacological modulation of subthalamic activity in Parkinson's disease. Exp Neurol 2004;189(2):369–79.

Portet F, Ousset PJ, Visser PJ, Frisoni GB, Nobili F, Scheltens P, et al. MCI Working Group of the European Consortium on Alzheimer's Disease (EADC). Mild cognitive impairment (MCI) in medical practice: a critical review of the concept and new diagnostic procedure. Report of the MCI Working Group of the European Consortium on Alzheimer's Disease. J Neurol Neurosurg Psychiatry 2006;77(6):714–8.

Raichle ME, Gusnard DA. Intrinsic brain activity sets the stage for expression of motivated behavior. J Comp Neurol 2005;493(1):167–76.

Raichle ME, Mintun MA. Brain work and brain imaging. Annu Rev Neurosci 2006;29:449–76.

Rodriguez G, Copello F, Nobili F, Vitali P, Perego G, Nobili F. EEG spectral profile to stage Alzheimer's disease. Clin Neurophysiol 1999a;110:1831–7.

Rodriguez G, Nobili F, Copello F, Vitali P, Gianelli MV, Taddei G, et al. 99mTc-HMPAO regional cerebral blood flow and quantitative electroencephalography in Alzheimer's disease: a correlative study. J Nucl Med 1999b;40:522–9.

Rodriguez G, Vitali P, De Leo C, De Carli F, Girtler N, Nobili F. Quantitative EEG changes in Alzheimer patients during long-term donepezil therapy. Neuropsychobiology 2002;46(1):49–56.

Rossini PM, Del Percio C, Pasqualetti P, Cassetta E, Binetti G, Dal Forno G, et al. Conversion from mild cognitive impairment to Alzheimer's disease is predicted by sources and coherence of brain electroencephalography rhythms. Neuroscience 2006;143(3):793–803.

Rubin EH, Morris JC, Grant FA, Vendegna T. Very mild senile dementia of the Alzheimer type I. Clinical assessment. Arch Neurol 1989;46(4):379–82.

Rumelhart DE, Smolensky P, McClelland JL, Hinton GE. Schemata and sequential thought processes in PDP models. In: McClelland JL, Rumelhart DE, editors. Exploration in the microstructure of cognition 1986;Vol. II. Cambridge, MA: The MIT Press; 1986.

Scheltens P, Fox N, Barkhof F, De Carli C. Structural magnetic resonance imaging in the practical assessment of dementia: beyond exclusion. Lancet Neurol 2002;1(1):13–21.

Stern Y. Cognitive reserve and Alzheimer disease. Alzheimer Dis Assoc Disord 2006;20(2):112–7.

Tanaka Y, Hanyu H, Sakurai H, Takasaki M, Abe K. Atrophy of the substantia innominata on magnetic resonance imaging predicts response to donepezil treatment in Alzheimer's disease patients. Dement Geriatr Cogn Disord 2003;16(3):119–25.

Vialette F, Chicocki A, Dreyfus G, Toshimitsu M, Gervais R. Early detection by blind source separation, time frequency, and bump modelling of EEG signals. In: Proceedings of the 15th international conference on artificial neural networks: biological inspirations (ICANN'05). Springer; Warsaw, Poland: 2005;3696:683–92.

Villa AE, Tetko IV, Dutoit P, Vantini G. Non-linear cortico-cortical interactions modulated by cholinergic afferences from the rat basal forebrain. Biosystems 2000;58(1–3):219–28.

Zaudig M. A new systematic method of measurement and diagnosis of "mild cognitive impairment" and dementia according to ICD-10 and DSM-III-R criteria. Int Psychogeriatr 1992;4:203–19.